ISSN 1330-3651 (Print), ISSN 1848-6339 (Online) https://doi.org/10.17559/TV-20240527001680
Original scientific paper

Design of 100 kW Three-Phase Bidirectional AC-DC Matrix Converter for Fast Charging of Electric Vehicles

Jamal ABRAS*, Ahmet Mete VURAL

Abstract: This study addresses the demand for efficient and rapid charging solutions driven by the rise in electric vehicle (EV) adoption. It presents the design and simulation of a 100 kW bidirectional AC-DC matrix converter tailored for fast EV charging. Key aspects include the converter's three-phase matrix architecture, control strategies utilizing PI controllers and PWM, and the management of bidirectional power flow. Additionally, the study evaluates power, voltage, and current performance on both AC and DC sides, explores battery charging and discharging characteristics, and assesses total harmonic distortion (THD) across multiple simulation cases. The findings contribute a comprehensive design approach for high-power bidirectional converters, enhancing the EV charging infrastructure and supporting advancements in sustainable transportation technologies.

Keywords: bidirectional AC-DC matrix converter; control strategies; electric vehicle; fast charging; power electronics

1 INTRODUCTION

With the accelerating global shift towards sustainable transportation, electric vehicles (EVs) have emerged as a crucial solution to mitigate greenhouse gas emissions and reduce dependency on fossil fuels. EVs utilize high-efficiency electric motors and controllers, contributing to a cleaner and more environmentally friendly transportation system [1-5]. As the number of electric vehicles (EVs) increases, the demand for efficient and robust charging infrastructures becomes critical to support their adoption. Rapid charging solutions are vital for improving the practicality and acceptance of EVs. A key component of this infrastructure is the power converter, which facilitates the transfer of electrical energy between the grid and the vehicle's battery during peak demand periods [6]. Traditional charging methods often encounter limitations regarding charging speed and adaptability to varying grid conditions. In contrast, AC-DC matrix converters (MCs) have garnered considerable interest as a novel solution. They leverage the intrinsic benefits of MCs, including high power density, compact architecture, variable input power factor, sinusoidal input current, and four-quadrant operation [7]. An AC-DC MC is a bidirectional, one-stage, current-source buck rectifier that is extensively utilized in battery energy storage systems, EVs, renewable energy generation, and AC-DC microgrids [8]. Although significant progress has been made in AC-DC converters for EV applications, there is still a gap in the development of high-power bidirectional converters using three-phase matrix architectures. This research addresses the limitations of current charging infrastructures by designing a 100kW bidirectional AC-DC matrix converter (MC) for fast electric vehicle (EV) charging. The proposed converter enhances charging performance by enabling faster energy transfer and improving system through the elimination of an intermediate DC-DC stage, simplifying the overall system architecture. Moreover, this study integrates a filter design that reduces THD to less than 4%, thus improving power quality, and optimizes control strategies to ensure stable bidirectional power flow, enabling energy transfer between the vehicle and the grid. In summary, this study differs from existing ones in that it focuses on the design of a high-power (100 kW) bidirectional AC-DC matrix converter with a single-stage topology that enhances power quality and eliminates the need for a DC-DC converter, thereby improving performance in electric vehicle fast charging applications. The remainder of this paper is organized as follows: Section 2 provides a thorough review of relevant literature, highlighting the existing state of bidirectional converters and their applications in EV charging. Section 3 outlines the proposed architecture and design considerations. Control strategies are detailed in Section 4. Results and analysis are presented in Section 5, followed by the conclusions in Section 6.

2 LITERATURE REVIEW

The challenges of energy shortages and environmental pollution have driven the push for sustainable solutions in the automotive sector. Electric Vehicles (EVs) and plug-in hybrid vehicles are widely seen as effective solutions to these problems [9, 10]. The increasing importance of Vehicle-to-Grid (V2G) technology is clear, as it is poised to play a crucial role in the EV market, allowing vehicles to not only consume but also return energy to the grid [11], [12]. EVs represent a major pillar in the transition to sustainable energy, offering emission-free and silent transport options [13]. One of the major obstacles to wider adoption of EVs is the issue of long charging times and range anxiety. The design of fast DC charging stations is critical to address these concerns, enabling quick and convenient charging solutions for today's users [14] as shown in Tab. 1.

Table 1 Charging modes characteristics

Type	Location	Power Level / kW	Charging Duration
Level 1: 120 VAC	On-board	1.2-2.0	18 hours
Level 2 (low): 208-240 VAC	On-board	2.8-3.8	8 hours
Level 2 (high): 208-240 VAC	On-board	6-15	4 hours
Level 3: 208-240 VAC	Off-board	> 15-96	20-50 min
Level 3: DC Charging: 600 VDC	Off-board	> 15-240	20-50 min

DC fast charging systems are categorized into two levels: Level 1 systems, which provide a power rating of

up to 40 kW, and Level 2 systems, offering a power rating up to 100 kW [15]. Depending on the station's power rating, these systems can charge an EV in under an hour [16]. A critical component of any EV charging system is the converter, which converts electrical power from AC to DC form for battery charging. The efficiency, cost, and complexity of charging systems are heavily dependent on the design of these converters. Most systems employ a two-stage conversion process involving an AC-DC converter followed by a DC-DC converter [17]. However, this approach often leads to larger, more complex systems with decreased efficiency due to high power losses in the diodes and other components [18, 19]. In contrast, more advanced converter topologies, such as current source rectifiers, are explored in [20, 21], which allow better power quality (PQ) but still come with challenges like higher power losses and the need for bulky electrolytic capacitors. Previous studies have shown significant weaknesses in existing designs, including low power ratings, complex control systems, and the necessity for two-stage DC-DC converters, which add to system complexity and energy losses while increasing costs. Additionally, many existing converters exhibit high Total Harmonic Distortion (THD), adversely affecting power quality and system stability. Recent research focuses on bidirectional single-converter topologies that reduce size and complexity while maintaining the necessary charging/discharging characteristics for V2G applications [22] as shown in Fig.1.

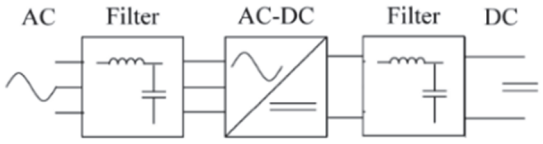

Figure 1 Topologies of buck type AC-DC conversion single-stage

These topologies provide greater efficiency and are better suited for the demands of modern EV infrastructures, including the integration of power electronics advancements such as bidirectional converters [23, 24]. Bidirectional converters are essential for V2G technology as they allow energy to flow from the vehicle back to the grid during peak demand periods. For effective V2G integration, converters need to possess certain key characteristics: a high-quality sinusoidal current at the grid interface and a configurable power factor (ideally unity), the power flow can change quickly to fulfill the space limitation in EVs, high efficiency, simple design, and high-power density. Voltage-source-type Pulse Width Modulation (PWM) rectifiers are frequently employed for their ability to allow bidirectional energy flow and improve input current quality, though they often require additional chopper circuits, which add to the system's cost and complexity [25]. Matrix Converters (MCs), a new class of converters, have gained significant attention due to their potential to address the limitations of current high-power EV chargers. MCs offer several advantages, including reduced component count, direct power conversion without the need for bulky capacitors, and the ability to achieve high power density with improved efficiency [26]. Additionally, MCs allow bidirectional power flow and provide superior control over power quality, which makes them ideal for V2G applications. The study in [23, 24] demonstrates how MCs, particularly when employing Space Vector PWM (SVPWM) techniques, can maintain unity power factor and provide high-quality DC output voltage. These capabilities are critical for high-power EV charging stations, as they ensure efficient, rapid energy transfer while minimizing power losses and harmonic distortions. In particular, the use of a three-phase bidirectional AC-DC MC for a 100 kW DC fast charging station offers the potential to meet the growing demands of EV infrastructure [26].

Despite advancements in converter technology, there remain significant gaps in the design of high-power, bidirectional AC-DC converters for fast electric vehicle (EV) charging. Existing research primarily focuses on lower power ratings or specific aspects of bidirectional converters, highlighting the need for comprehensive solutions tailored to fast charging infrastructures. To address these limitations, this study proposes a detailed design for a 100 kW bidirectional AC-DC Matrix Converter (MC) that will be validated through simulation. In addition, two charging modes - constant current charging and constant voltage charging - will be examined, as this single-stage topology is particularly well-suited for Vehicle-to-Grid (V2G) applications. All design components, including the control systems, will be developed and verified within a simulation environment optimized for power electronics and control applications. Key design considerations for the bidirectional AC-DC MC include achieving low harmonic distortion (approaching an ideal sinusoidal waveform) at the input, ensuring unity power factor operation, and minimizing output ripple. To address harmonic distortion, a passive filter design (of either the LC or LCL type) will be implemented at the converter's input. This research aims to provide an essential solution for the next generation of sustainable transportation technologies.

3 PROPOSED EV CHARGING SYSTEM

The proposed EV charging system is illustrated in Fig. 2. This section provides a detailed insight into the components, topology, and operational principles of the system architecture. The system is fed from a low voltage three-phase AC source through an input filter. This filter is a second-order LC filter. It consists of two energy storage components: an inductor (L) and a capacitor (C), which is used to prevent the transmission of high-frequency harmonic currents produced by the converter into the grid and to protect the converter from high-frequency harmonics present in the grid. The heart of the system is a three-phase MC with direct AC-AC conversion capability without the need for an intermediate DC link.

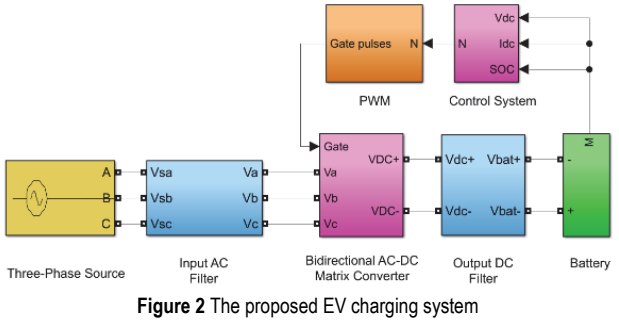

Figure 2 The proposed EV charging system

This topology reduces the number of components, enhancing overall system reliability and efficiency. The output filter is connected between the MC output and the EV battery to smooth the charging current. The battery is lithium-ion (Li-ion) type, nominal voltage 600 V, maximum capacity 228 Ah, cut-off voltage 450 V, fully charged voltage 645 V, nominal discharge current 100 A. On the other hand, the control system is designed to effectively control the charging and discharging modes. In this study, two charging modes are considered. These are constant current charging and constant voltage charging modes. A traditional Pulse Width Modulation (PWM) approach is used to provide fine digital control over switching commutation within power converters. Its simplicity has led to its adoption across a variety of power converter topologies, establishing its broad use in industrial applications. PWM has various advantages, including reduced filtering requirements, less computing overhead, and more effective power transmission [27].

The MC Topology includes a set of bidirectional switches, forming a matrix of controllable paths for power flow. These switches, implemented using advanced power electronics devices, enable precise control over the conversion process. The most popular controllable static switches used in the design of power electronic converters are displayed below in Tab. 2.

Table 2 Main controllable switches comparison

Device	Power Capability	Switching Speed
MOSFET	Low	Fast
IGCT	High	Slow
IGBT	Medium	Medium

The insulated-gate bipolar transistor (IGBT) tends to be the best option for the design of the MC circuit in terms of cost. An IGBT converter typically operates with an efficiency of around 90% [28]. The AC/DC MC must operate in two modes for V2G applications: charging mode and discharging mode. In essence, this converter enables power to flow in both directions. However, no such device is available; instead, unidirectional devices are used to construct a bidirectional switch cell.

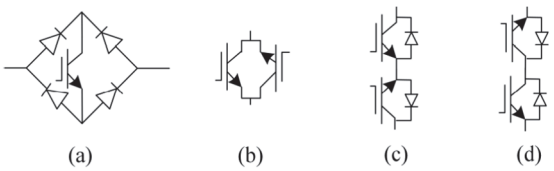

Figure 3 Different bidirectional switch cell (a) diode bridge bidirectional switch cell (b) anti-parallel reverse blocking IGBT (c) common emitter anti-parallel IGBT (d) common collector anti-parallel IGBT, [33]

Generally, there are four different ways to build bidirectional switch cells as shown in Fig. 3 [29, 30]. Fig. 3a depicts a diode bridge switch containing an IGBT and four diodes, allowing current flow in both directions with high conduction loss and uncontrolled current direction. Alternatively, Fig. 3b shows an anti-parallel reverse blocking IGBT that controls current flow but experiences high voltage and current spikes during switching. Fig. 3c features a common-emitter anti-parallel IGBT switch with two IGBTs and two diodes, offering controlled current direction and reduced conduction loss. Lastly, Fig. 3d presents a common collector switch with similar conduction loss to the common emitter. The common emitter anti-parallel IGBT configuration has the potential to use one isolated power supply for two IGBT gate drivers. Two IGBTs are used to provide the current path, and two diodes are connected to provide the reverse blocking capability. The current direction can be controlled, and only one IGBT and one diode are conducted at each conduction path. Therefore, the common-emitter configuration is preferable for a MC [31, 32]. The AC/DC MC can be streamlined to a simple topology as illustrated in Fig. 4 $S1$(a, b), $S2$(a, b), … $S6$(a, b). Two IGBTs with anti-parallel gates typically implement the bidirectional switches. A free-wheeling diode and a common emitter coupled in series [34]. To stop high frequency harmonic currents generated by the converter from entering the grid and to prevent the grid's high frequency harmonics from interfering with the converter, a second-order LC input filter is employed.

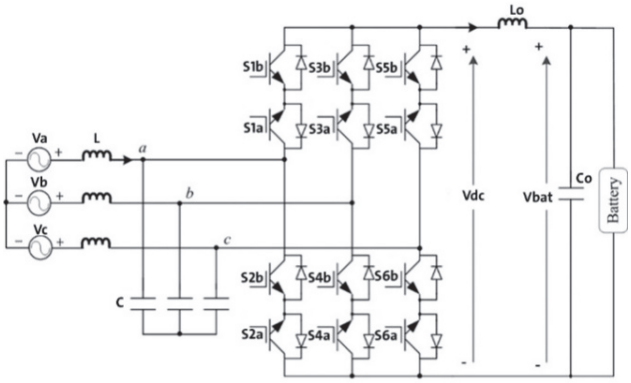

Figure 4 Topology of AC/DC MC

The output filter's inductor, Lo, and capacitor, Co, are there to smooth out the charging current. The AC/DC matrix converter must operate in both charging and discharging modes in V2G applications. This converter essentially permits bidirectional power flow. By turning all the switches $S1$b, $S2$b, ..., $S6$b OFF while it is operating in charging mode, comparatively, when it discharges mode the switches $S1$a, $S2$a, ..., $S6$a are all turned OFF. PWM modulation is illustrated in Fig. 5, which shows the power topology of the MC. The mathematical model of the converter can be obtained by combining the states of six bidirectional switches into a single vector. Hence, the output voltage $V = [Vp - Vn]$ directly depends on the input voltages (Va, Vb, and Vc) and the current switch states ($S1$ to $S6$) [27] as shown in Tab. 3.

The Pulse Width Modulation (PWM) technology is applied in this type of modulation, having various advantages such as reduced filtering requirements, fewer mathematical computations, and better transmission of effective power. The modulation system has two essential components: the first is responsible for implementing the PWM system, generating a modulated signal that matches the reference waveform via a control system. The second section focuses on dividing the three-phase input source to identify different voltage areas defined by various line-to-line voltage combinations. For a three-phase input source, identifying distinct voltage regions is critical for choosing the devices to be switched using Tab. 3. The segmentation of the input source is shown as a function of the provided voltage values over time. These unique sections are

represented by the variables $X1$, $X2$, ..., $X6$, which are generated by binary comparators in logic circuit 1 that detect whether the phase voltage exceeds the subsequent phase. Finally, using the information provided by the control system (N) and the data from the comparator blocks identifying the sectors of the three-phase input source ($X1$, $X2$, ..., $X6$), the 12 switching signals ($S1$a, $S1$b, ..., $S6$a, $S6$b) can be obtained, and by applying logic circuit 2 (OR), the switching signals ($S1$, $S2$, ..., $S6$) are derived for the MC converter.

Table 3 Space vector of AC/DC MC

	Output		Sector	Trigger Pulses					
	Vp	*Vn*	*X*	*S*1	*S*2	*S*3	*S*4	*S*5	*S*6
1	*Va*	*Vb*	6	1	0	0	0	0	1
2	*Va*	*Vc*	6	1	0	0	0	0	1
3	*Vb*	*Vc*	6	1	0	0	0	0	1
4	*Vb*	*Va*	2	0	1	0	0	0	1
5	*Vb*	*Vc*	2	0	1	0	0	0	1
6	*Va*	*Vc*	2	0	1	0	0	0	1
7	*Vb*	*Va*	3	0	1	0	1	0	0
8	*Vb*	*Vc*	3	0	1	0	1	0	0
9	*Vc*	*Va*	3	0	1	0	1	0	0
10	*Vc*	*Va*	1	0	0	1	1	0	0
11	*Vc*	*Vb*	1	0	0	1	1	0	0
12	*Vb*	*Va*	1	0	0	1	1	0	0
13	*Vc*	*Va*	5	0	0	1	0	1	0
14	*Vc*	*Vb*	5	0	0	1	0	1	0
15	*Va*	*Va*	5	0	0	1	0	1	0
16	*Va*	*Vb*	4	1	0	0	0	1	0
17	*Va*	*Vc*	4	1	0	0	0	1	0
18	*Vc*	*Vb*	4	1	0	0	0	1	0

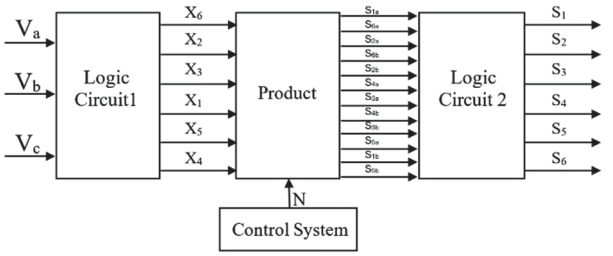

Figure 5 Topology of PWM modulation

Input AC filter is designed to ensure compliance with grid standards and reduce harmonic distortion, an input AC filter is incorporated. This filter minimizes high-frequency components and enhances power quality during AC-DC conversion. A passive LC filter is applied in the AC/DC MC as can be seen in Fig. 6a. The method for designing a passive LC filter is a general concept based on the principles of designing simple LC filters [35], as shown by Eq. (1), which provides the fundamental relationship between inductance (L), capacitance (C), and the desired cutoff frequency.

$$f_C = \frac{1}{2\pi\sqrt{LC}} \tag{1}$$

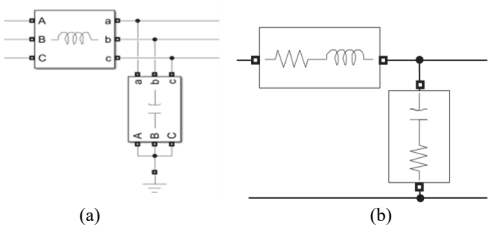

Figure 6 Input AC Filter (a), Output DC Filter (b)

The cutoff frequency (fc) is determined by considering the grid frequency (50 Hz) and the target for harmonic reduction. Specifically, the objective is to attenuate harmonics above the 3rd order, necessitating the attenuation of frequencies above 150 Hz (3 × 50 Hz). Consequently, the cutoff frequency (fc) is established at 125 Hz, with an initial estimate for the capacitance (C) set at 4 mF. The necessary inductance (L) is derived using equation 1 for the cutoff frequency of an LC filter, where (fc) and (C) are known parameters. (L) = 0.4 mH, in selecting components, commercially available inductors and capacitors that closely match the calculated values are chosen. For instance, a selection might include a 0.4 mH inductor and a 4 mF capacitor. It is crucial to ensure that the selected inductance value (L) remains sufficiently small to avoid impeding the flow of current from the grid to the MC and to prevent a significant voltage drop across the inductor. This consideration helps maintain the MC input voltage at parity with the grid voltage.

Output DC filter is integrated to smooth the pulsations of the rectified current during EV charging. This filter assists in shaping the output waveform and suppressing harmonics, contributing to the charging system's efficiency and stability. A well-designed output filter is required for minimal current ripple and for proper dynamic response. An LC filter is applied in the AC/DC MC as can be seen in Fig. 6b. The design of output filter is based on two considerations: the dynamic response of the system and the suppression of current ripple. The output current response may become slower when using a large LC filter, which is frequently employed to reduce output current ripple. Therefore, a compromise between these two factors needs to be made. The method for designing a passive LC filter is a general concept based on the principles of designing simple LC filters [35] as shown by Eq. (1). The cutoff frequency fc is established at 300 Hz, with an initial estimate for the capacitance C set at 6 μF inductance L is 50 mH and with capacitance C set at 10 μF inductance L is 90 mH . The values are obtained by trial and error for 3% current ripple when a capacitor of 10 μF and an inductor of 90 mH are used, as the battery presents large capacitive characteristics and has very stable voltage, C can be very small or even removed [34, 36].

4 PROPOSED CONTROL STRATEGIES

The control system employs a combination of Proportional-Integral (PI) controllers. The PI controllers regulate the AC-DC conversion processes. Control schemes have been created to improve the quality and performance of EV charging systems. The control strategies outlined for the 100 kW bidirectional AC/DC MC are crucial for ensuring efficient and reliable energy conversion in both AC-DC and DC-AC modes. These strategies adapt to the power requirements of the grid and the battery's state of charge (SOC) to optimize performance. Fig.7 describes the overall diagram of the proposed control scheme; the soft switching and conversion components are controlled. These converters can employ any modulation techniques such as SVPWM or SPWM - that was created for inverters. The converter operates in three modes: charging/discharging, constant current charging (CC), and constant voltage charging

(CV). CC and CV modes serve as maintenance modes to safeguard the battery from damage due to excessive charge/discharge. A feedback control loop is necessary to DC control for bidirectional AC-DC MC. The AC side current is directly influenced by the DC current, simplifying active power control. DC current is regulated by adjusting DC voltage or the modulation index N. The system output is the DC output voltage Vdc, current Idc, and SOC. The error signal is identified while the converters are under control by comparing the DC output current in CC charging mode Idc with a reference current Idc-ref and the DC output voltage in CV charging mode Vdc with a reference voltage Vdc-ref. To create a sample, this error is utilized. The PWM used to drive the switches in the converter is created using this sample waveform. Voltage source current control in CC charging mode or voltage control in CV charging mode are the two methods used to control switching signals. It serves as feedback in several control strategies, including sliding mode control, PID control, and PI controller. In this research, the Proportional-Integral (PI) controller was selected due to its suitability for electric vehicle charging applications. The PI controller provides quick responses and precise control, enhancing system stability and reducing steady-state errors through its integral component, which improves overall efficiency. It is particularly ideal for systems requiring rapid responses and high precision, such as electric vehicle charging. Additionally, PI controllers are straightforward to implement in digital systems, making them easier and quicker to design and execute. While other options like PID controllers exist, the PI controller is sufficient for this context, as the derivative action may not be necessary for enhancing performance. Using the PI controller also simplifies the design while increasing reliability. This choice is further supported by its successful application in various studies on electric vehicle charging, confirming it as a reliable and effective solution [37, 38].

A Proportional-Integral (PI) controller regulates the DC bus voltage Vdc during AC-DC conversion. It compares the actual Vdc with a reference voltage Vdc-ref, adjusts bidirectional switch duty cycles to maintain a stable output and regulates current charging. This precise control accommodates variations in battery SOC and charging demands. The charging control system is unplugged during the discharging mode.

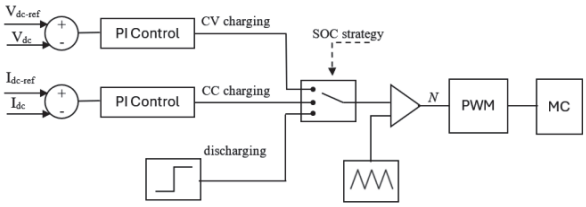

Figure 7 The proposed control strategies in this study

In our study, the reference charging voltage was established at 635 volts, ensuring it surpasses the nominal voltage of the battery yet remains below its full firing voltage. This selection ensures optimal charging conditions while safeguarding against overvoltage. Similarly, the reference charging current was determined not to surpass the maximum charging current specified by the battery, which in this case is 200 A. This cautious approach ensures safe charging by mitigating risks of excessive current flow.

5 SIMULATION RESULTS AND ANALYSIS

A comprehensive set of experiments was conducted under various conditions to evaluate the performance of the 100kW bidirectional AC/DC MC included real-time monitoring of critical parameters such as voltage, current, and power flow direction in the simulation environment to validate the suggested method. Tab. 4 contains a list of the parameters of the AC/DC MC used in simulation, while Fig. 2 displays the schematic representation of the same. In our study, we will present three scenarios for battery charging: Charging the battery from 10% to 90% using constant current charging, charging the battery from 10% to 90% using constant voltage charging, discharging the battery from 100% to 90%.

Table 4 Parameters used for AC/DC MC simulation

Parameters	Value
Three-Phase AC Source	400 Volt –50 Hz
Input AC Filter	0.4 mH –4mF
Output DC Filter	90 mH –10μF –0.001Ω
Switching and Sampling frequency	25 kHz
Battery	100 kW, 100-228 Ah, 600 V Lithium-Ion. Max charge current 200 A

Charging the battery from 10% to 90% using constant current charging: Fig.8 presents the simulated electrical parameters at the AC side of the EV charging station in constant current charging mode.

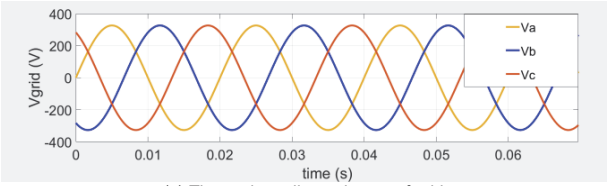

(a) Three-phase line voltages of grid

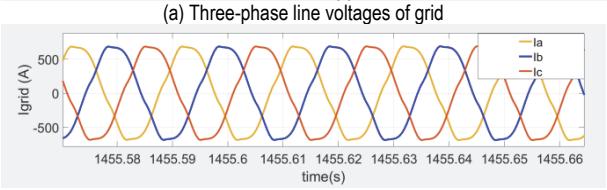

(b) Three-phase line currents of grid

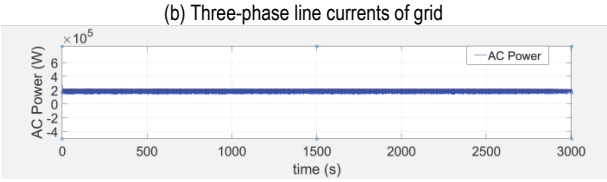

(c) Active power drawn from AC grid

(d) Reactive power drawn from AC grid

Figure 8 The electrical parameters at the AC side in CC charging mode

Active power of about 185 kW flows from the grid to the rectifier side and a reactive power of 0 kVAR flows in the system as shown in Fig. 8c-d respectively. Power factor is 1 and THD is 3%.

At the DC side, 630 V output DC voltage, 200 A output DC current, and an output DC power of about 126 kW are maintained, allowing the charging of the battery as shown in Fig. 9.

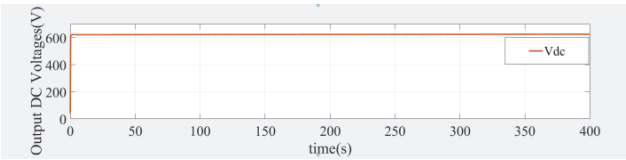

(a) Output DC voltages

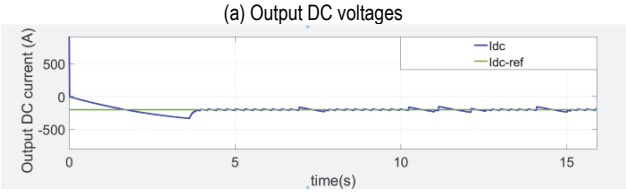

(b) Output DC current

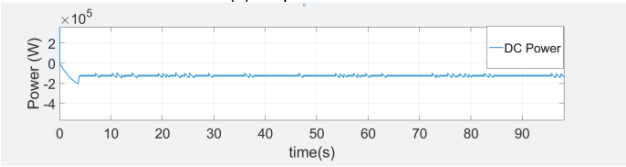

(c) Output DC power

Figure 9 The electrical parameters at the DC side in CC charging mode

As for the battery, Fig. 10 shows charging the battery from 10% to 90%. It is seen that the charging time takes around 55 minutes with 630 V DC and 200 A DC, provided by the converter.

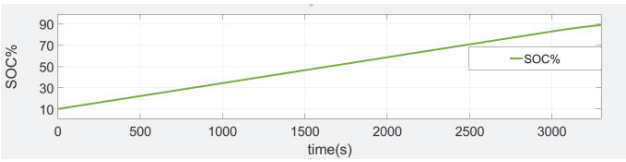

(a) Battery charging SOC

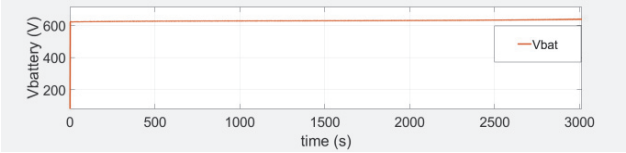

(b) Battery charging voltage (V)

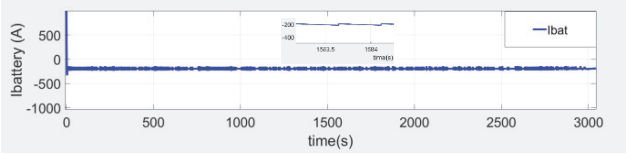

(c) Battery charging currents (A)

Figure 10 The battery charging from SOC 10% to 90% in CC mode: The SOC, the charging current, the charging voltage.

Charging the battery from 10% to 90% using constant voltage charging: the charging process when there is no current control and charging is constant voltage charging (CV). Fig. 11 presents the simulated electrical parameters at the AC side of the EV charging station in constant voltage mode. Active power varies significantly at the beginning of charging, starting from 400 kW to reach a small value at the end of charging flows from the grid to the rectifier side and a reactive power of 0 kVAR flows in the system as shown in Fig. 11c-d respectively. Power factor is 1 and THD about 3%.

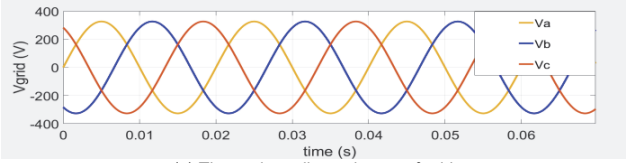

(a) Three-phase line voltages of grid

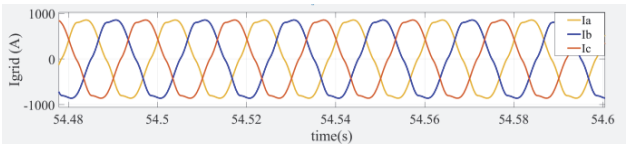

(b) Three-phase line currents of grid

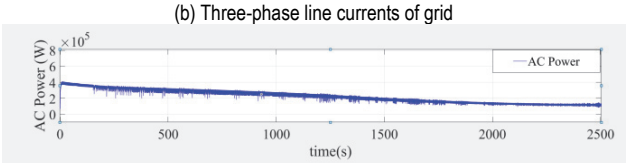

(c) Active power drawn from AC grid

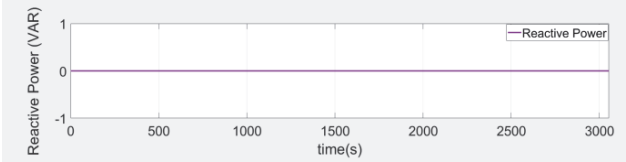

(d) Reactive power drawn from AC grid

Figure 11 The electrical parameters at the AC side in CV charging mode

Fig. 12 shows the DC side, the value of the charging current at the beginning of charging is approximately 630 A and decreases during the charging process to reach a low value close to zero at the end of the charging as shown in Fig. 12b. DC power varies significantly at the beginning of charging, starting from 400 kW to reach a small value at the end of charging.

(a) Output DC voltages

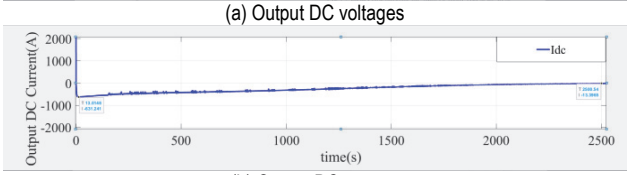

(b) Output DC current

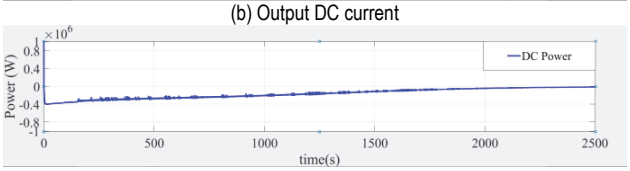

(c) Output DC power

Figure 12 The electrical parameters at the DC side in CV charging mode

As for the battery, Fig. 13 shows charging the battery from 10% to 90%. It is seen that the charging time takes around 40 minutes with 635 V DC, and the battery current at the beginning of charging is approximately 630 A.

During the charging the current decreases to reach a low value close to zero at the end of the charging process provided by the converter. Charging with a constant voltage (CV) has several problems, including power instability and significant changes in the charging current value during the process. The current starts from a very high value that exceeds the maximum charge current, causing damage to the battery. Determining the reference value for the constant voltage (Vdc-ref) is difficult. In our study, we chose a reference value close to the battery's full charging voltage, resulting in a very high initial charging current. Choosing a lower reference voltage stops the charging process early, preventing the battery from fully charging.

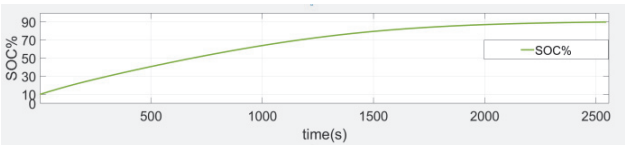

(a) Battery charging SOC

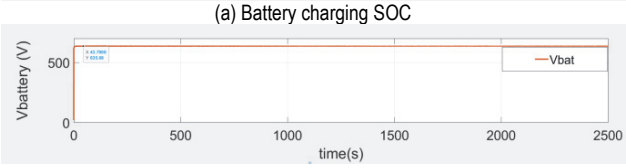

(b) Battery charging voltage (V)

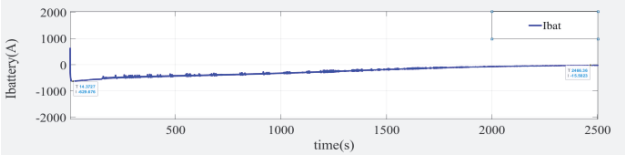

(c) Battery charging currents (A)

Figure 13 The battery charging from SOC 10% to 90% in CV mode: The SOC, the charging current, the charging voltage.

Discharging the battery from 100% to 90%: bi-directional capability of V2G operation. Fig. 14 shows the electrical parameters at the AC side in discharging mode.

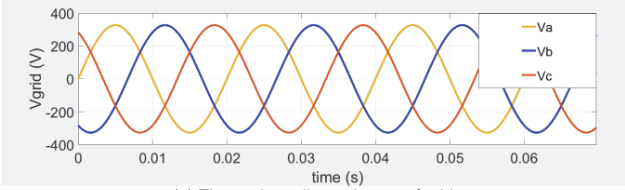

(a) Three-phase line voltages of grid

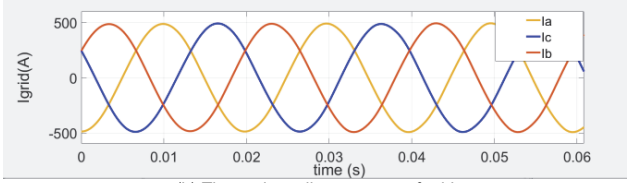

(b) Three-phase line currents of grid

Figure 14 The electrical parameters at the AC side in discharging mode

Fig. 15 shows discharging the battery from 100% to 90%, as the voltage is constant 635 V, the current is 150 A resulting in the battery power returning to the grid. Depending on the needs and operational conditions of the system, the system's bidirectionality may be beneficial.

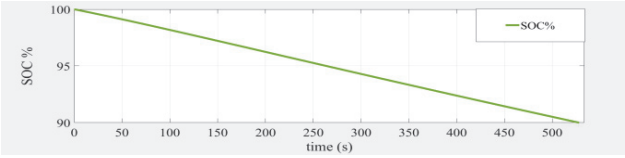

(a) Battery discharging SOC

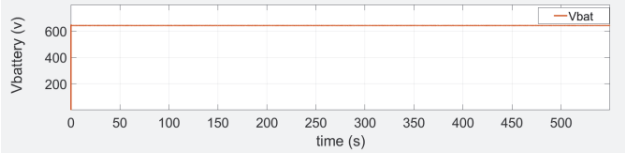

(b) Battery discharging voltage (V)

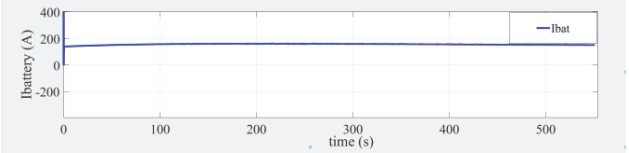

(c) Battery discharging current (A)

Figure 15 The battery discharging from SOC 100% to 90%

6 CONCLUSION

The development of the 100kW bidirectional AC-DC matrix converter for electric vehicle (EV) fast charging represents a notable advancement in power electronics and sustainable transportation. This converter simplifies the system by reducing components and enhancing reliability while facilitating direct AC-DC and DC-AC conversion without an intermediary DC link. The integration of a Proportional-Integral (PI) controller ensures efficient and precise control, enabling rapid and reduced total harmonic distortion. This innovation significantly enhances EV charging infrastructure, paving the way for a more efficient and sustainable future in electric transportation.

7 REFERENCES

[1] Fuinhas, J. A., Koengkan, M., Leitão, N. C., Nwani, C., Uzuner, G., Dehdar, F., Relva, S., & Peyerl, D. (2021). Effect of Battery Electric Vehicles on Greenhouse Gas Emissions in 29 European Union Countries. *Sustainability*, *13*(24), 13611. https://doi.org/10.3390/su132413611

[2] Wang, Y.N., Zhang, Z.J., Ping, A., Wang, R.J., & Gong, D.Q. (2024). Optimizing electric vehicle charging strategies using multi-layer perception-based spatio-temporal prediction of charging station load, *Advances in Production Engineering & Management, 19*(4), 443-459. https://doi.org/10.14743/apem2024.4.518

[3] Tang, M. C., Cao, J., Gong, D. Q., Xue, G., & Khoa, B. T. (2024). Simulation Modelling of Electric Vehicle Charging Recommendations Based on Q-Learning. *International Journal of Simulation Modelling, 23*(3), 495-506. https://doi.org/10.2507/IJSIMM23-3-CO11

[4] Park, H., Jin, S. (2020). Electric Vehicle Routing Problem with Heterogeneous Vehicles and Partial Charge. *International Journal of Industrial Engineering and Management, 11*(4), 215–225. https://doi.org/10.24867/IJIEM-2020-4-266

[5] Gong, D., Tang, M.; Liu, S., Xue, G., & Wang, L. (2019). Achieving sustainable transport through resource scheduling: A case study for electric vehicle charging stations, *Advances in Production Engineering & Management, 14*(1), 65-79. https://doi.org/10.14743/apem2019.1.312

[6] Kumar, D., Nema, R. K., & Gupta, S. (2020). A comparative review on power conversion topologies and energy storage system for electric vehicles. *International Journal of Energy Research*, *44*(10), 7863-7885. https://doi.org/10.1002/er.5353

[7] Mahmud, T. & Gao, H. (2023). AC-DC Matrix Converter Topologies: AComprehensive Review. *TechRxiv*. https://doi.org/10.36227/techrxiv.24062076.v1

[8] Habib, S., Ehsan, F., Liu, H., Nadeem, M. H., Abbas, F., & Numan, M. (2021). A comprehensive topological assessment of power electronics converters for charging electric vehicles. *Flexible Resources for Smart Cities*, 133-183. https://doi.org/10.1007/978-3-030-82796-0_7

[9] Alanazi, F. (2023). Electric vehicles: benefits, challenges, and potential solutions for widespread adaptation. *Applied Sciences*, *13*(10), 6016. https://doi.org/10.3390/app13106016

[10] Zhao, J., Xi, X., Na, Q., Wang, S., Kadry, S. N., & Kumar, P. M. (2021). The technological innovation of hybrid and plug-in electric vehicles for environment carbon pollution control. *Environmental Impact Assessment Review*, *86*, 106506. https://doi.org/10.1016/j.eiar.2020.106506

[11] Mojumder, M. R. H., Ahmed Antara, F., Hasanuzzaman, M., Alamri, B., & Alsharef, M. (2022). Electric vehicle-to-grid (V2G) technologies: Impact on the power grid and battery. *Sustainability*, *14*(21), 13856.

https://doi.org/10.3390/su142113856
[12] Zagrajek, K., Paska, J., Sosnowski, Ł., Gobosz, K., & Wróblewski, K. (2021). Framework for the introduction of vehicle-to-grid technology into the Polish electricity market. *Energies*, *14*(12), 3673. https://doi.org/10.3390/en14123673
[13] Shen, J., Wang, L., & Zhang, J. (2021). Integrated scheduling strategy for private electric vehicles and electric taxis. *IEEE Transactions on Industrial Informatics*, *17*(3), 1637-1647. https://doi.org/10.1109/TII.2020.2993239
[14] Zhang, H., Qiu, J., & Wang, Y. (2021). Planning strategy of fast-charging stations in coupled transportation and distribution systems considering human health impact. *International Journal of Electrical Power & Energy Systems*, *133*, 107316. https://doi.org/10.1016/j.ijepes.2021.107316
[15] Antao, R., Goncalves, T., & Martins, R. E. (2013). Modular design of dc-dc converters for EV battery fast-charging. *International Conference on Renewable Energies and Power Quality (ICREPQ'13)*. https://doi.org/10.24084/repqj11.360
[16] Khalid, M., Ahmad, F., & Panigrahi, B. K. (2021). Design, simulation, and analysis of a fast-charging station for electric vehicles. *Energy Storage*, *3*(6), e263. https://doi.org/10.1002/est2.263
[17] Kempton, W. & Tomić, J. (2005). Vehicle-to-grid power implementation: From stabilizing the grid to supporting large-scale renewable energy. *Journal of Power Sources*, *144*(1), 280-294. https://doi.org/10.1016/j.jpowsour.2004.12.022
[18] Soeiro, T., Friedli, T., & Kolar, J. W. (2012). Three-phase high power factor mains interface concepts for electric vehicle battery charging systems. *Applied Power Electronics Conference and Exposition (APEC) 2012 Twenty-Seventh Annual IEEE*, 2603-2610. https://doi.org/10.1109/APEC.2012.6166190
[19] Kang, M., Enjeti, P. N., & Pitel, I. J. (1999). Analysis and design of electronic transformers for electric power distribution systems. *IEEE Transactions on Power Electronics*, *14*(6), 1133-1141. https://doi.org/10.1109/63.803407
[20] Chapman, D., James, D., & Tuck, C. J. (1993). A high density 48 V 200 A rectifier with power factor correction: an engineering overview. *Telecommunications Energy Conference, INTELEC '93 15th International*, *1*, 118-125. https://doi.org/10.1109/INTLEC.1993.373788
[21] Krishnamoorthy, H. S., Garg, P., & Enjeti, P. N. (2012). A matrix converter-based topology for high power electric vehicle battery charging and V2G application. *IECON 2012 - 38th Annual Conference on IEEE Industrial Electronics Society*, 2866-2871. https://doi.org/10.1109/IECON.2012.6389440
[22] Liu, R., Dow, L., & Liu, E. (2011). A survey of PEV impacts on electric utilities. *IEEE PES Innovative Smart Grid Technologies Conference*, 1-8. https://doi.org/10.1109/ISGT.2011.5759171
[23] Holmes, D. G. & Lipo, T. A. (1992). Implementation of a controlled rectifier using AC-AC matrix converter theory. *IEEE Transactions on Power Electronics, 7*(1), 240-250. https://doi.org/10.1109/63.124596
[24] Garcia, R., Espi, J. M., Sanchis, E., Esteve, V., Jordan, J., & Maset, E. (2004). A DSP-controlled four-quadrant AC-DC matrix converter with high-frequency isolation. *Conference Proceedings - IEEE Applied Power Electronics Conference and Exposition - APEC*, *2*, 1194-1199. https://doi.org/10.1109/APEC.2004.1295974
[25] Sanchis-Kilers, E., Carrasco, J. A., de la Calle, R., Espi, J. M., & Ejea, J. B. (2001). High-frequency bi-directional three-phase rectifier with power factor correction. *IEEE*, *3*, 1303-1308. https://doi.org/10.1109/PESC.2001.954300
[26] Wei, H., Zhang, Y., Wang, Y., Hua, W., Jing, R., & Zhou, Y. (2022). Planning integrated energy systems coupling V2G as a flexible storage. *Energy*, *239*(Part B), 122215. https://doi.org/10.1016/j.energy.2021.122215
[27] Rivera, M., Rojas, S., Restrepo, C., Muñoz, J., Baier, C., & Wheeler, P. (2020). Control techniques for a single-phase matrix converter. *Energies*, *13*(23), 6337. https://doi.org/10.3390/en13236337
[28] Investigation on storage technologies for intermittent renewable energies: evaluation and recommended R&D strategy. (2003). *Investire-Network*, Contract N° ENK5-CT-2000-20336.
[29] Klumpner, C., Nielsen, P., Boldea, I., & Blaabjerg, F. (2002). New solutions for a low-cost power electronic building block for matrix converters. *IEEE Transactions on Industrial Electronics*, *49*(2), 336-344. https://doi.org/10.1109/41.993266
[30] Wheeler, P. W., Rodriguez, J., Clare, J. C., Empringham, L., & Weinstein, A. (2002). Matrix converters: a technology review. *IEEE Transactions on Industrial Electronics*, *49*(2), 276-288. https://doi.org/10.1109/41.993260
[31] Klumpner, C. & Blaabjerg, F. (2006). Using reverse-blocking IGBTs in power converters for adjustable-speed drives. *IEEE Transactions on Industry Applications*, *42*(3), 807-816. https://doi.org/10.1109/TIA.2006.872956
[32] Takei, M., Naito, T., & Ueno, K. (2003). The reverse blocking IGBT for matrix converter with ultra-thin wafer technology. *ISPSD '03: 2003 IEEE 15th International Symposium on Power Semiconductor Devices and ICs*, 156-159. https://doi.org/10.1109/ISPSD.2003.1225253
[33] Fang, F. (2021). PWM and control strategies for AC-DC matrix converters. *University of Alberta*. https://doi.org/10.7939/r3-462p-ts98
[34] Su, M., Wang, H., Sun, Y., Yang, J., Xiong, W., & Liu, Y. (2013). AC/DC matrix converter with an optimized modulation strategy for V2G applications. *IEEE Transactions on Power Electronics*, *28*(12), 5736-5745. https://doi.org/10.1109/TPEL.2013.2250309
[35] Mohan, N., Undeland, T. M., & Robbins, W. P. (2003). *Power electronics: converters, applications, and design*. John Wiley & Sons.
[36] Metidji, R., Metidji, B., & Mendil, B. (2013). Design and implementation of unity power factor fuzzy battery charger using ultra sparse matrix rectifier. *IEEE Transactions on Power Electronics*, *28*(5), 2269-2276. https://doi.org/10.1109/TPEL.2012.2211107
[37] Goyal, S. K., Gangil, G., & Saraswat, A. (2022). Simulation of solar-grid charging of electric vehicles using PI controller. *2022 2nd International Conference on Innovative Practices in Technology and Management (ICIPTM)*, 247-252. https://doi.org/10.1109/ICIPTM54933.2022.9754003
[38] Haque, M. R., Salam, K. M. A., & Razzak, M. (2023). A modified PI-controller based high current density DC-DC converter for EV charging applications. *IEEE Access*, *11*, 27246-27266. https://doi.org/10.1109/ACCESS.2023.3258181

Contact information:

Jamal ABRAS
(Corresponding author)
Electrical and Electronics Engineering Department,
Gaziantep University, Turkey
E-mail: jamalabras@gmail.com

Ahmet Mete VURAL
Electrical and Electronics Engineering Department,
Gaziantep University, Turkey
E-mail: mvural@gantep.edu.tr